ISSN: 2638-1559

madridge PUBLISHERS
Interconnecting Scientific World

International
Journal of Material Science and Research

Research Article

Open Access

Laser Metal Deposition of Aluminum 7075 Alloy

A Bhagavatam, A Ramakrishnan, VSK Adapa and **Guru P Dinda***

Department of Mechanical Engineering, Wayne State University, Detroit, MI 48202, USA

Article Info

***Corresponding author:**
Guru P Dinda
Department of Mechanical Engineering
Wayne State University
MI 48202
Detroit, USA
Phone: +1 313 577 1989
E-mail: dinda@wayne.edu

Received: September 5, 2018
Accepted: October 16, 2018
Published: October 23, 2018

Citation: Bhagavatam A, Ramakrishnan A, Adapa VSK, Dinda GP. Laser Metal deposition of Aluminum 7075 Alloy. *Int J Mater Sci Res.* 2018; 2(1): 50-55.
doi: 10.18689/ijmsr-1000108

Published by Madridge Publishers

Abstract

Additive manufacturing (AM) has become one of the most important research topics with its ability to manufacture a wide range of alloys like steel, nickel-based super alloys, titanium alloys, aluminum alloys, etc. Al 7075 is not a friendly alloy for laser metal deposition (LMD). This paper reports the successful development of LMD process for deposition of defect-free Al 7075 alloy. By preheating the substrate to 260°C the residual stress decreased and eliminated the hot/solidification cracks in the deposit. LMD is a rapid cooling process due to which the gas bubbles of Mg and Zn are trapped in the deposit. These are identified as gas porosity because of the partial evaporation of low boiling point elements like magnesium and zinc present in this alloy. The least porosity observed was 0.08% at 29 J/mm^2 of energy input. The SEM and EDS investigation of as-deposited Al 7075 revealed the segregation of Cu, Mg, and Zn rich phases along the interdendritic regions and grain boundaries. Cu, Mg, and Zn rich phases at the interdendritic regions dissolved into the α-Almatrix after heat treatment. The XRD scan of laser deposited Al 7075 revealed the presence of Al_2CuMg and $MgZn_2$ precipitation hardening phases.

Keywords: Additive Manufacturing; Laser Metal Deposition; Microstructure; Al 7075 Alloy

Introduction

Laser metal deposition (LMD) is an additive manufacturing process that utilizes a laser as a heat source for melting metal powder to form a 3D component layer-by-layer [1]. LMD is a directed energy deposition process, which is also known as solid freeform fabrication, laser solid forming, direct metal deposition, etc. LMD is a rapid solidification process, which results in a fine grain microstructure. It assists industries in manufacturing and repairing components with complex designs that cannot be processed through conventional manufacturing techniques. Processing of aluminum alloys by LMD receives attention from the automotive and aerospace industries [2-5]. Aluminum alloys have a high strength to weight ratio with excellent oxidation resistance. Al 7075 is one of the most commonly used heat treatable 7xxx series alloy with Zn, Cu, and Mg as primary alloying elements. Typically, it is used in aerospace applications including fuselage frames, bulkheads and wing skins [6]. It has good corrosion resistance, thermal conductivity, and machinability that promote the utilization of Al 7075 in aerospace industries [3,7-10]. The mechanical properties of Al 7075 can be improved with heat-treatment whose strength increases by the precipitation of $Mg(Zn,Cu,Al)_2$ phases [11]. Commonly T6 heat treatment is used to enhance the mechanical properties of this alloy [9]. The microstructure of cast and heat-treated Al-Zn-Mg-Cu alloys may form several intermetallic phases like η($MgZn_2$), S(Al_2CuMg), Al_2Cu, Al_7Cu_2Fe, $Al_2Mg_3Zn_3$, Mg_2Si [9,12].

One of the biggest challenges of processing of Al 7075 is hot tearing, which is a very common casting defect in 7xxx series aluminum alloys. Hot tearing is a crack formed in hot metal during cooling, caused by an improper pouring temperature or undue restraint. A large solidification range results in a greater chance for hot tearing as less liquid is available for interdendritic feeding when the material reaches the solidus or eutectic temperature [13]. Numerous studies have been reported on hot tearing and a solution is proposed by using a controlled diffusion solidification process [14].

Higher solidification cracking sensitivity of Al 7075 alloy weldments poses a challenge for several researchers. Generally, solidification cracking occurs when higher levels of thermal stress and solidification shrinkage are present during welding [13]. Al 7075 has large solidification temperature (*T*)range ($\Delta T = T_{liquidus} - T_{solidus}$) and is further increased because of non-equilibrium solidification and rapid cooling rates during LMD [13]. The primary methods for eliminating cracking in aluminum welds are to control weld metal composition through filler alloy additions. In practice, the solidification cracking sensitivity of aluminum alloy weldments is determined by the chemical composition and weld conditions. During welding of Al 7075, hot cracking may occur due to the liquation of $CuMgAl_2$ and Fe-rich particles surrounded with Cu_2FeAl within the solid solubility limit due to the high cooling rate [12].

Selective laser sintering (SLM) of Al 7075 alloy investigated by Reschetnik et al. [15] revealed that the cracks developed parallel to the building direction with poor mechanical properties. By coating pre-alloyed Al 7075 powder of particle size 40 µm with 1 vol% hydrogen stabilized zirconium nucleants eliminated cracking during SLM [16]. LMD process gives a lot of flexibility to customize and repair parts used in automobile and aerospace industries. LMD of 7xxx series aluminum alloys always remained a challenge. Al 7050 alloy is difficult to process with LMD because of low boiling point elements such as Mg and Zn present in it. Singh A et al. [2] gave an alternative solution to deposit Al 7050 by coating the metal powder with nickel. LMD processed nickel coated Al 7050 was free from porosity but displayed poor tensile ductility because of formation of brittle Al_3Ni intermetallic at the interdendritic boundaries. To improve the tensile properties, the deposit was friction stir processed. Froend M et al. [4] developed wire based LMD process parameters for Al 5087. This alloy consists of low boiling point element such as Mg in it. This causes porosity and residual stress because of rapid cooling in the LMD process. To overcome the problem of defect formation during LMD, substrate was preheated to reduce the thermal gradient and residual stresses in the deposit.

There is tremendous need to develop AM for Al 7xxx because of its limitless applications in the aerospace and automobile industry. It is vital to overcome the challenges faced by previous researchers like hot tearing and hot/ solidification cracking. The primary objective of this research is to systematically develop LMD process parameters (with different preheat temperatures of the substrate) for defect-free deposition of Al 7075 alloy. The mechanical properties and microstructural evolution of the as-deposited and heat-treated Al 7075 alloy are discussed.

Experimental Procedure

Laser metal deposition process

The gas atomized Al 7075 powder (ValimetInc) with -140/+325 mesh size is used in the current investigation. The powder composition is shown in table 1. Rolled Al 7075 plate of 150 mm × 50 mm × 25 mm dimensions was used as the substrate, as shown in figure 2. During LMD, the laser beam is focused at a point on the substrate, which forms a melt pool. The metal powder passes through the four jets of the nozzle converging at the same point of the focused laser beam delivering the metal powder simultaneously into the melt pool. Argon gas is used to carry the powder from the powder feeder into the melt pool to prevent oxidation. A CNC framework is utilized to control the movement of the laser head (consisting of nozzle and optics) as per the tool path created from the Computer-Aided Design (CAD) model [17].

The LMD experiments have been carried out using Synergy AM3018 machine with a 6-kW diode laser, with laser beam diameter of 2 mm and four beam jet nozzles. The samples are deposited with dimensions of 25 mm × 25 mm in a cross-hatch pattern.

Table 1. Chemical composition of as-received Al 7075 powder in wt %.

	Al	Cu	Mg	Mn	Fe	Si	Zn	Ti	Cr
Al 7075	Bal.	1.63	2.20	0.01	0.07	0.15	5.11	0.01	0.23

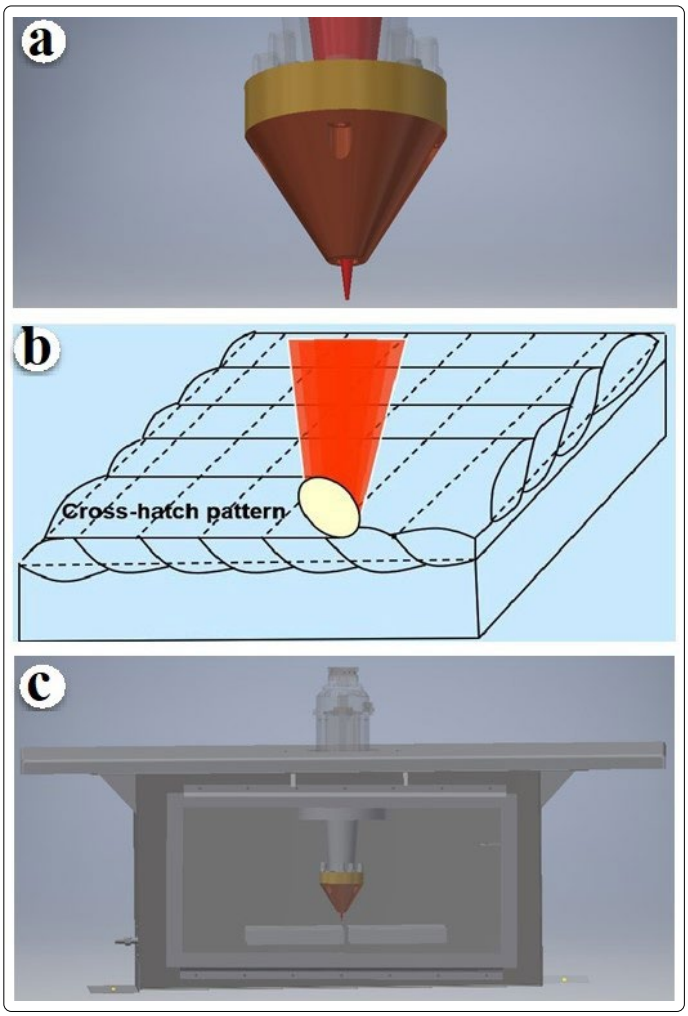

Figure 1. Schematics of (a) Laser metal deposition nozzle, (b) Cross-hatch deposition pattern, and (c) Argon chamber with nozzle head.

The deposition was carried out in an argon chamber with less than 2% of Oxygen, as schematically shown in figure 1c. Laser power had to be more than usual to melt aluminum alloys due to the high thermal conductivity. Various parameters (laser power, travel speed, powder flow rate) were optimized to achieve near 100% dense deposition. Travel speed plays a crucial role in maintaininga stable melt pool thereby enhancing clad quality. The Taguchi L9 matrix used to optimize the process parameters is shown in table 2.

Table 2. Optimized laser deposition process parameters for Al 7075

LMD parameters for Al 7075 (Sample#)	Laser Power (Watt)	Travel Speed (mm/min)	Powder feed rate (g/min)	Gas flow rate (SCFH)	
				Carrier gas	Shielding gas
1	900	500	1.66	5	5
2	1200	500	1.66	5	5
3	1500	500	1.66	5	5
4	900	750	1.66	5	5
5	1200	750	1.66	5	5
6	1500	750	1.66	5	5
7	900	1000	1.66	5	5
8	1200	1000	1.66	5	5
9	1500	1000	1.66	5	5

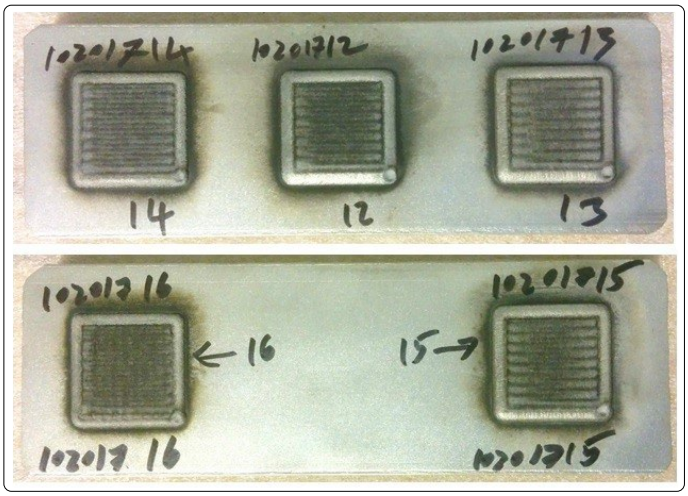

Figure 2. Al 7075 deposition on Al 7075 rolled substrate.

Microstructural analysis

The deposited coupons are cross-sectioned and polished to evaluate the percentage of porosity using an optical microscope. For the microstructural investigation, samples are etched in a solution of 100 ml H_2O+25 ml HNO_3+15 ml HCl+10 ml HF for 5-10 s and further rinsed in methanol and dried. The hardness of these samples was tested with Vickers hardness tester using 100 g load for a dwell time of 10s. X-ray diffraction investigation is conducted using Bruker D2 Phaser diffractometer with Cu target in the standard θ–2θ geometry from 20° to 105° to examine the phases in the as-deposited and heat-treated condition. The microstructural analysis is carried out using a JSM 7600 scanning electron microscope (SEM), and elemental composition is analyzed through energy dispersive spectroscopy (EDS) investigation. T6 heat treatment was carried out to increase the mechanical properties of the as-deposited samples. Al 7075 was solution heat treated at 480°C for 4 h and then quenched in water followed by aging at 120°C for 24 h. The optical and SEM micrographs revealed the hot/solidification cracks in phase 1 (no substrate preheating) samples. To overcome the hot/solidification cracks observed during phase 1, the substrate is pre-heated to 260°C before deposition. The same phase 1 optimization parameter window is used to deposit 25 mm × 25 mm coupons and similar tests are conducted on phase 2 (substrate preheated to 260°C) samples.

Results and Discussion

Figures 3a and 3b shows the optical micrographs of Al 7075 deposits when the substrate was at room temperature and with preheating the substrate at 260°C. Porosity in this material is mainly concentrated on the region closer to the surface in the top part of the deposit. This is because of partial evaporation of low boiling point elements, such as Mg and Zn present in the deposit. The liquid melt pool solidifies before the gas completely escapes from the melt pool. Whereas, preheating the substrate to 260°C in phase 2 (substrate preheated to 260°C) reduced the percentage of porosity compared to phase 1 (no substrate preheating) samples, as observed in figures 3b and 3d. Preheating the substrate gives more time for solidification of the melt pool, thereby; gas bubbles of Zn and Mg had sufficient time to escape from the liquid melt pool without being trapped as observed in phase 1. Figure 3a reveals the hot/solidification cracks in phase 1 forming due to the high cooling rate in laser metal deposition process. Solidification cracking occurs when higher levels of thermal stress and solidification shrinkage are present during deposition. These cracks are entirely eliminated in the phase 2 sample by preheating the substrate to 260°C, as shown in figure 3b.

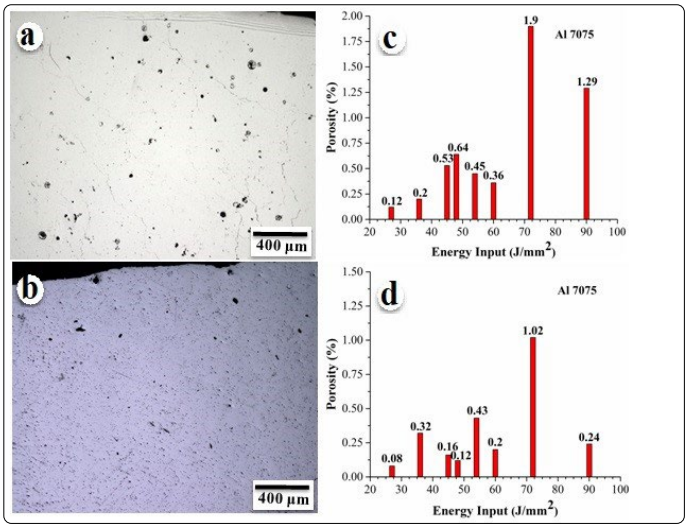

Figure 3. (a) Optical micrograph of as-deposited Al 7075 sample #5 produced in phase 1 (no substrate preheating), (b) Optical micrograph of as-deposited Al 7075 sample #5 produced in phase 2 (substrate preheated to 260°C), (c) Porosity vs. Energy input of as-deposited Al 7075 samples produced in phase 1, and (d) Porosity vs. Laser energy input of as-deposited Al 7075 samples produced in phase 2.

Tables 3 and 4 list the percentage of porosity and number of cracks at different energy input in phase 1 and phase 2, respectively. The following equation for Energy input (J/mm^2)=laser power (Watt)/[travel speed (mm) × laser beam diameter (mm)] was used for calculation. Phase 1 samples have more porosity and cracks compared with phase 2 samples. The least porosity in both phase 1 and phase 2 is observed at a laser power of 900 W and 1000 mm/min travel speed. Cracks are completely eliminated in phase 2 except sample number 8.

Figures 3c and 3d show the porosity vs. energy density of phase 1 and phase 2 samples, respectively. It is observed that the porosity increases with an increase in energy density because of the substantial evaporation of Mg and Zn during LMD. At highest energy input, porosity in phase 2 decreases to 0.2% because the Mg and Zn gasses escaped significantly from the melt pool before solidification begins.

Table 3. Porosity % and the number of cracks in as-deposited Al 7075 samples produced in phase 1.

Scan Speed	900 W	1200 W	1500 W
500 mm/min	Porosity:0.45% No. of cracks: low (1-5)	Porosity: 1.9% No. of cracks: Med. (1-5)	Porosity: 1.289% No. of cracks: High (5-10)
750 mm/min	Porosity: 0.27% No. of cracks: High (10+)	Porosity: 0.64% No. of cracks: Med. (1-5)	Porosity: 0.36% No. of cracks: High (10+)
1000 mm/min	Porosity: 0.12% No. of cracks: High (10+)	Porosity: 0.23% No. of cracks: High (10+)	Porosity: 0.53% No. of cracks: High (10+)

Table 4. Porosity % and the number of cracks in as-deposited Al 7075 samples produced in phase 2.

Scan Speed	900 W	1200 W	1500 W
500 mm/min	Porosity: 0.43% No cracks	Porosity: 1.02% No cracks	Porosity: 0.24% No cracks
750 mm/min	Porosity: 0.25% No cracks	Porosity: 0.12% No cracks	Porosity: 0.2% No cracks
1000 mm/min	Porosity: 0.08% No cracks	Porosity: 0.32% Few cracks	Porosity: 0.16% No cracks

Microstructural investigation

Microstructural investigation of the as-deposited and heat-treated sample is carried out using SEM and EDS analysis. Figures 4a and 4b shows crack propagation along dendrite and grain boundaries. These hot/solidification cracks are formed due to large residual stresses formed during subsequent deposition of multiple layers. Interdendritic regions observed in the as-deposited condition in phase 1 and phase 2 was not present after heat-treatment. Figure 4d exhibits that Cu and Zn rich phases formed along the dendrite and grain boundaries in as-deposited condition. The Cu and Zn rich phases observed in the as-deposited condition dissolved into the matrix during heat treatment as observed in figure 4e. The EDS analysis of the as-deposited and heat-treated sample shown in figures 4d and 4e reveal that there is a decrease in the zinc and magnesium percentage compared to the powder composition. The boiling point of Al is 2470°C, which is significantly higher than Mg (1091°C) and Zn (907°C). This explains that Mg and Zn partially evaporated during deposition.

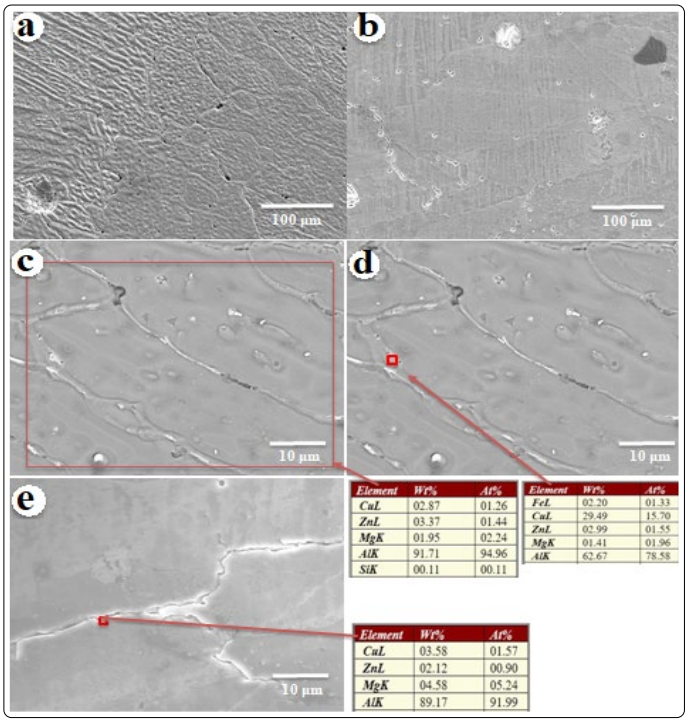

Figure 4. SEM micrographs of the (a) as-deposited Al 7075, (b) heat-treated Al 7075, (c,d) EDS investigation of as-deposited Al 7075, and (e) EDS investigation of heat treated Al 7075 sample #5 produced in phase 1 (no substrate preheating).

Figures 5a and 5b shows the high magnification SEM and EDS images of phase 2 samples of the as-deposited and heat treated samples. Mg, Zn, and Cu rich phases segregated at the dendrite boundaries similar to the phase 1 samples. However, the level of segregation is lower in phase 2 compared to phase 1 samples. Preheating the substrate to 260°C caused low thermal gradient during deposition of consecutive layers and consequently resulted in less segregation of Cu, Mg, and Zn in the dendrite boundaries. It can be clearly seen from the figure 5a that high volume of the bright Cu, Mg- and Zn rich phases observed in the as-deposited condition dissolved into the matrix during solution treatment and formed a very low volume of strengthening precipitates during aging as shown in figure 5b. Moreover, there is an increase in the grain size after heat treatment. From figure 5c it is observed that there is a decrease in the zinc and magnesium percentage as compared to the powder composition. This explains that Mg and Zn partially evaporated during deposition.

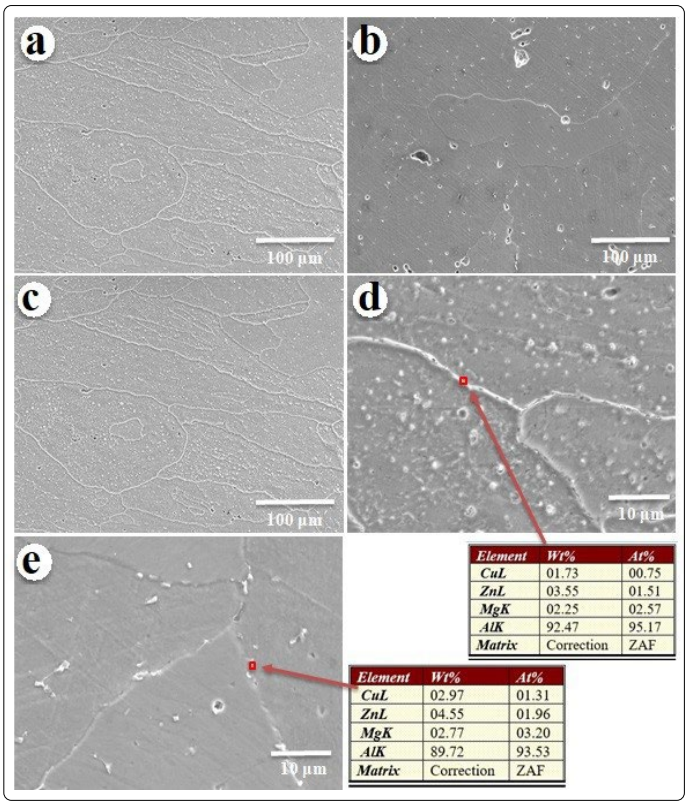

Figure 5. SEM micrographs of the (a) as-deposited Al 7075, (b) heat-treated Al 7075, (c, d) EDS investigation of as-deposited Al 7075, and (e) EDS investigation of heat treated Al 7075 sample #5 produced in phase 2 (substrate preheated to 260°C).

X-ray diffraction analysis

Figures 6a and 6b shows the XRD plots of the as-deposited and heat-treated samples produced in phase 1 and phase 2. There are only two intermetallic phases Al_2CuMg and $MgZn_2$ with α-Al formed in the as-deposited condition in both phase 1 and phase 2 samples, whereas, the intensity of $MgZn_2$ phase increased in the heat-treated samples.

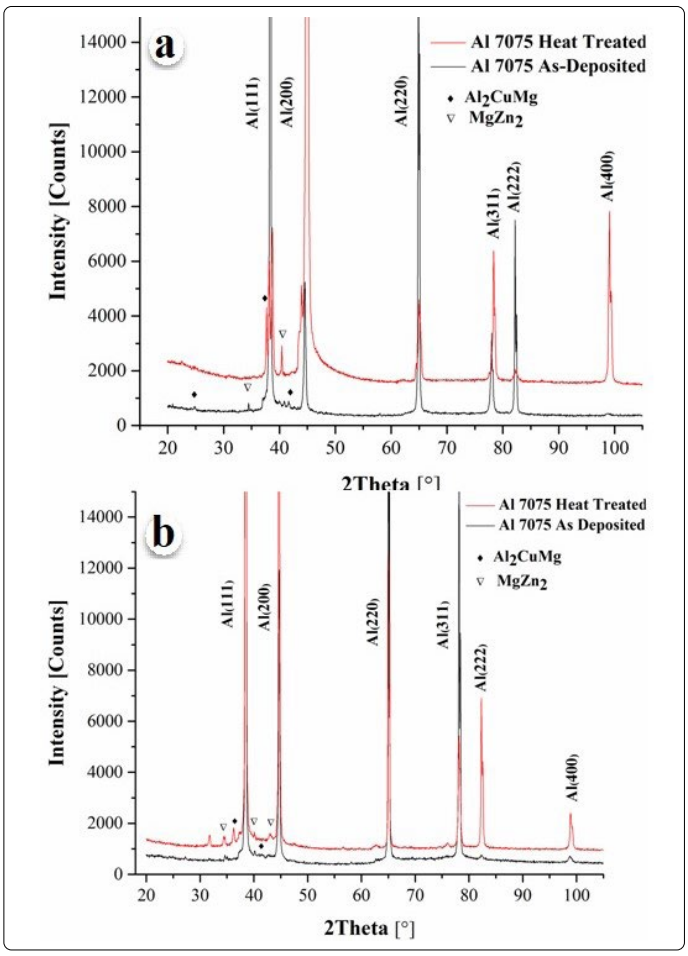

Figure 6. (a) XRD plots of the as-deposited and heat-treated Al 7075 sample #5 produced in phase 1, and (b) XRD plot of as-deposited and heat-treated Al 7075 sample #5 produced in phase 2.

Microhardness investigation

Hardness vs. energy density of Al 7075 in the as-deposited condition of phase 1 and phase 2 samples are shown in figures 7a and 7b. Minor variation in the hardness of the sample is observed after heat treatment. The hardness of the phase 1 sample in the as-deposited and heat treated condition is found to be 93.9 HV and 96.7 HV, respectively. The hardness of the phase 2 sample in the as-deposited and heat treatment condition is 104.0 HV and 101.7 HV, respectively. According to the literature during casting, the hardness of heat-treated Al 7075 should be around 160-175HV [18,19]. However, this is not the case for a laser metal deposited sample because of substantial evaporation of low boiling point material such as Zn and Mg during LMD.

The present investigation demonstrates that Al 7075 can be successfully fabricated using LMD. Formation of porosity in the as-deposited specimen is mainly due to the evaporation of Mg and Zn during processing in phase 1. Mg and Zn have a low boiling temperature compared to Al. Consequently, Mg and Zn gas are trapped in the deposit. This porosity percentage increases with an increase in energy input. Al 7075 has maximum porosity at the highest energy input resulting in higher cooling rates and hence increasing the evaporation of Mg and Zn in the deposit. Similarly, in phase 2 porosity increases till the energy input reaches 70 J/mm^2 and then decreases rapidly. At an input energy density of 90 J/mm^2, more heat is accumulated resulting in lower thermal gradient. Henceforth, Mg and Zn gasses escape before the solidification of the melt pool. X-ray diffraction investigation shows the as-deposited Al 7075 has Al_2CuMg and $MgZn_2$ phases and intensity of these phases increased after heat-treatment. From the SEM and EDS investigation, it is observed that the cracks propagated along the interdendritic regions and grain boundaries. From these results and microstructural investigation, it is observed that hot/solidification cracking of these alloys is due to high residual stress developed during subsequent deposition of multiple layers. The cracking susceptibility is reduced due to the preheating of the substrate before deposition in phase 2 experiments. Microhardness of the as-deposited samples of these materials is low compared to the literature because of high cooling rates (10^3–10^5 K/s) associated with this process. As a result, the strengthening elements remain as a solid solution in the α-Al matrix resulting in a lower hardness of the as-deposited samples. To increase the hardness, the as-deposited samples are heat treated according to the T6 heat treatment cycle. There is a slight increase in hardness after post-deposition heat-treatment due to the formation of strengthening precipitates during aging.

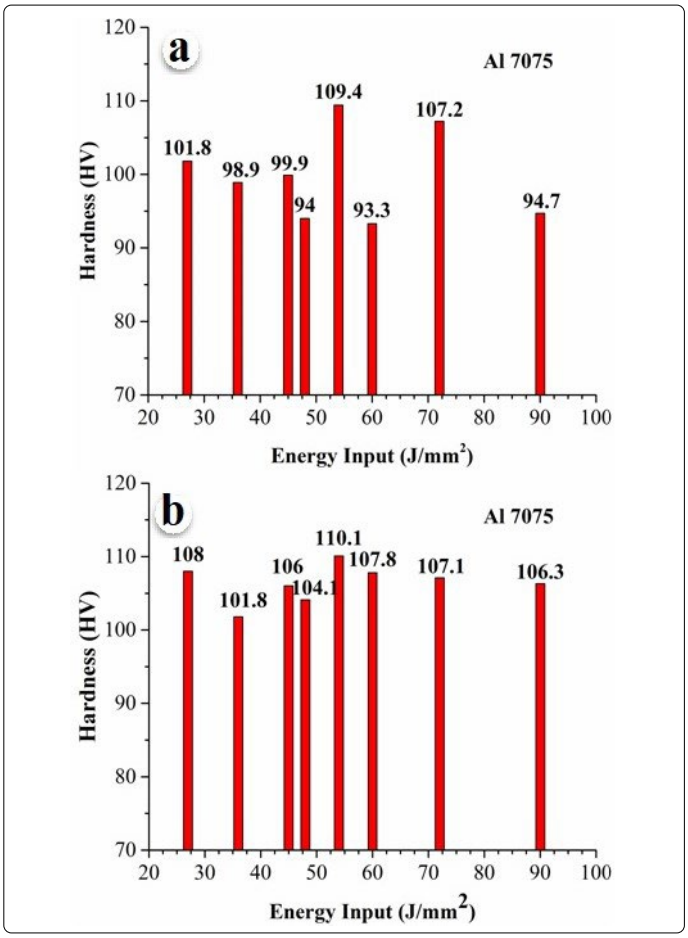

Figure 7. Specific energy input vs. hardness plot of as-deposited Al 7075 samples (a) produced in phase 1, and (b) produced in phase 2.

Conclusion

The present investigation demonstrates that 99.9% dense Al 7075 alloy can be successfully deposited by LMD. Porosity observed in these alloys is mainly due to the magnesium and zinc present in the composition. Hot cracks are seen in phase 1 samples. However, preheating the substrate eliminated the cracks

in phase 2 samples. X-ray diffraction investigation revealed the presence of α-Al, Al_2CuMg, and $MgZn_2$ phases in the laser deposited Al 7075. SEM and EDS investigation revealed the formation of cracks in the phase 1 sample that propagated along the dendrite and grain boundaries. The hardness variations were very low after heat-treatment in both phase 1 and phase 2 specimens. From this investigation, it can be concluded that the propagation of hot/solidification cracks in Al 7075 during LMD can be eliminated by preheating the substrate at 260°. In the future, tensile testing will be carried out to investigate the yield strength, ultimate tensile strength, and ductility of defect-free as-deposited and heat-treated Al 7075 specimens. Further research is required to design and develop LMD parts using Al 7075 alloy.

Acknowledgment

Our special thanks to Synergy Additive Manufacturing LLC and Technical director Aravind Jonnalagadda for his guidance and support during this project. Financial support from the Michigan Corporate Relations Network and Synergy Additive Manufacturing LLC is gratefully acknowledged.

References

1. Tan H, Hao D, Al-Hamdani K, Zhang F, Xu Z, Clare AT. Direct metal deposition of TiB2/AlSi10Mg composites using satellited powders. *Materials Letters*. 2018; 214: 123-126. doi: 10.1016/j.matlet.2017.11.121
2. Singh A, Ramakrishnan A, Baker D, Biswas A, Dinda GP. Laser metal deposition of nickel coated Al 7050 alloy. Journal of Alloys and Compounds. *Journal of Alloys and Compounds*. 2017; 719: 151-158. doi: 10.1016/j.jallcom.2017.05.171
3. Dinda GP, Dasgupta AK, Bhattacharya S, Natu H, Dutta B, Mazumder J. Microstructural Characterization of Laser-Deposited Al 4047 Alloy. *Metallurgical and Materials Transactions A*. 2013; 44(5): 2233-2242. doi:10.1007/s11661-012-1560-3
4. Froend M, Riekehr S, Kashaev N, Klusemann B, Enz J. Process development for wire-based laser metal deposition of 5087 aluminium alloy by using fibre laser. *Journal of Manufacturing* Processes. 2018; 34: 721-732. doi: 10.1016/j.jmapro.2018.06.033
5. Caiazzo F, Alfieri V, Argenio P, Sergi V. Additive manufacturing by means of laser-aided directed metal deposition of 2024 aluminium powder: Investigation and optimization. *Advances in Mechanical Engineering*. 2017; 9(8): 1-12. doi: 10.1177/1687814017714982
6. Hayat F. Effect of aging treatment on the microstructure and mechanical properties of the similar and dissimilar 6061-T6/7075-T651 RSW joints. *Materials Science and Engineering: A*. 2012; 556: 834-843. doi: 10.1016/j.msea.2012.07.077
7. Zuo H, Li H, Qi L, Zhong S. Influence of Interfacial Bonding between Metal Droplets on Tensile Properties of 7075 Aluminum Billets by Additive Manufacturing Technique. *Journal of Materials Science & Technology*. 2016; 32(5): 485-488. doi: 10.1016/j.jmst.2016.03.004
8. Singh SS, Guo E, Xie H, Chawla N. Mechanical properties of intermetallic inclusions in Al 7075 alloys by micropillar compression. *Intermetallics*. 2015; 62: 69-75. doi: 10.1016/j.intermet.2015.03.008
9. Zou XL, Yan H, Chen XH. Evolution of second phases and mechanical properties of 7075 Al alloy processed by solution heat treatment. *Transactions of Nonferrous Metals Society of China*. 2017; 27(10): 2146-2155. doi: 10.1016/S1003-6326(17)60240-1
10. Sreenivasa Rao KV, Govindaraju. Sliding wear Behavior of Cast Al-7075 Alloy Reinforced with MgO Particulates. *Materials Today: Proceedings*. 2017; 4(10): 11096-11101. doi: 10.1016/j.matpr.2017.08.071
11. Dabrowski J, Bruhis M, Kish JR. Effect of Corrosion on the Strength of Fillet arc Welded Cu-Lean AA7xxx Joints. Tms 141st Annual Meeting & Exhibition - Supplemental Proceedings, Vol 2: Materials Properties, Characterization, and Modeling. Warrendale: Minerals, Metals & Materials Soc. 2012; 437-444.
12. Huang C, Kou S. Liquation mechanisms in multicomponent aluminum alloys during welding. *Welding Journal*. 2002; 81: 211S-222S.
13. Fulcher BA, Leigh DK, Watt TJ. Comparison of AlSi10Mg and Al 6061 processed through DMLS. In: Proceedings of the Solid Freeform Fabrication (SFF) Symposium. Austin, TX, USA. 2014.
14. Ghiaasiaan R, Zeng X, Shankar S. Controlled Diffusion Solidification (CDS) of Al-Zn-Mg-Cu (7050): Microstructure, heat treatment and mechanical properties. *Materials Science and Engineering: A*. 2014; 594: 260-277. doi: 10.1016/j.msea.2013.11.087
15. ReschetnikW, Brüggemann JP, Aydinöz ME, et al. Fatigue crack growth behavior and mechanical properties of additively processed EN AW-7075 aluminium alloy. Procedia Structural Integrity. 2016; 2: 3040-3048. doi: 10.1016/j.prostr.2016.06.380
16. Martin JH, Yahata BD, Hundley JM, Mayer JA, Schaedler TA, Pollock TM. 3D printing of high-strength aluminium alloys. *Nature*. 2017; 549(7672): 365-369. doi: 10.1038/nature23894
17. Dinda GP, Dasgupta AK, Mazumder J. Evolution of Microstructure in Laser deposited Al–11.28%Si alloy. *Surface and Coatings Technology*. 2012; 206(8): 2152-2160. doi: 10.1016/j.surfcoat.2011.09.051
18. Clark R, Coughran B, Traina I, et al. On the correlation of mechanical and physical properties of 7075-t6 al alloy. Engineering Failure Analysis. 2005; 12(4): 520-526. doi: 10.1016/j.engfailanal.2004.09.005
19. Mahathaninwong N, Plookphol T, Wannasin J, Wisutmethangoon S. T6 heat treatment of rheocasting 7075 Al alloy. *Materials Science and Engineering: A*. 2012; 532: 91-99. doi: 10.1016/j.msea.2011.10.068